Power System Technology
ISSN:1000-3673

Received: 16-11-2025 Revised: 05-12-2025 Accepted: 30-01-2026

Reliability Assessment of Bullet Train System under Multi Uncertainty Scenarios using MILP Benders Decomposition Framework

P V Rajesh Varma and Shaik Affijulla

Department of Electrical Engineering
National Institute of Technology Meghalaya
Sohra, East Khasi Hills, Meghalaya, 793108, India
pesingirajeshvarma@gmail.com, shaik.affijulla@nitm.ac.in

Abstract:- High speed bullet trains require uninterrupted traction power, yet existing renewable integrated railway models do not quantify reliability under minute-wise grid outage conditions. This paper presents a multiscenario optimisation framework that evaluates outage driven reliability degradation and determines cost effective PV-battery support for uninterrupted train operation. Scenario 1, defined as stochastic Benders reliability assessment, analyses the black out sensitivity over the full system journey at randomised load and solar profiles. Scenario 2, referred as segment based Benders reliability assessment, enables segment level planning, adaptive sizing under realistic load and solar profiles. The dynamic Benders formulation achieves 98.95% reduction in Expected Energy Not Supplied (EENS) in Scenario 1 and 98.13% reduction in Loss of Load Probability (LOLP) in Scenario 2 compared with fixed optimised sizing. Scenario 3, a strategic joint cost reliability Mixed Integer Linear Programming (MILP) framework evaluates the trade-off between cost and reliability under budget and EENS constraints. The proposed framework integrates outage modelling, renewable dispatch and reliability optimisation into a unifed methodology. Simulation results confirm that proposed optimisation framework maintains traction continuity while enabling economically effcient renewable sizing for next generation high speed rail corridors.

Keywords: *Grid outages, Bullet train, reliability indices, PV generation, battery sizing.*

1. Introduction

High speed bullet train systems represent a transformative advancement in modern transportation infrastructure, with traction power demands that vary significantly during acceleration, cruising and braking phases. Any interruption in power supply particularly grid outages can compromise operational safety and passenger comfort. Ensuring resilient and sustainable energy support is therefore critical for uninterrupted operation. Integrating renewable sources such as photovoltaic (PV) generation, battery energy storage systems (BESS) and coordinated substation support offers a promising pathway to enhance traction power reliability under blackout conditions.

Prior research in rail transport has largely focused on intelligent train control and operational optimisation. Energy effcient train control strategies using Soft Actor Critic (SAC) learning [1] and Deep Deterministic Policy Gradient (DDPG) algorithms [2] have been proposed to minimise traction energy consumption. Maintenance oriented studies have introduced periodic

Power System Technology
ISSN:1000-3673
Received: 16-11-2025 Revised: 05-12-2025 Accepted: 30-01-2026

scheduling frameworks for high speed trains [3] and degradation based reliability modelling using Piecewise Deterministic Markov Processes (PDMP) has been applied to train wheels [4]. These studies overlook the coordination required between PV generation, battery storage, and substations to sustain traction power when the grid supply becomes unstable.

Energy optimisation frameworks have also been applied to railway systems. For instance, train scheduling models considering line slopes, speed constraints, and braking behaviour have been used to reduce traction energy consumption [5], while coordinated power rail interaction models have been proposed to enhance supply demand balancing in high speed train fleets [6]. Demand response programs have been integrated into metro systems to support grid side flexibility [7]. MILP (Mixed Integer Linear Programming) based sizing of PV (Photo Voltaic) and BESS (Battery Energy Storage Systems) for traction substations has demonstrated the feasibility of renewable supported rail operation [8]. These existing models fail to incorporate the spatial temporal nature of a moving high speed train, where outage severity depends on the train's position relative to substations.

Recent developments in renewable integrated railway systems have examined the use of PV, wind and hybrid energy storage for long term cost reduction and emission savings [9], [10]. Case studies on high speed rail corridors highlight the benefits of Hybrid Energy Storage Systems (HESS) for improving operational efficiency [11, [12], [13]. Additional work has explored regenerative braking energy recovery using BESS [14] and robust optimisation of co-phase traction substations under PV and load uncertainties [15]. Furthermore, prior work does not analyse minute level outage effects or determine how PV-BESS dispatch should adapt dynamically to maintain traction power throughout the journey.

Parallel research in microgrids provides valuable insights due to the shared reliance on PV-BESS coordination. Time series renewable management strategies for isolated microgrids [16] and hybrid evolutionary MILP optimisation frameworks for energy scheduling under uncertainty [17] demonstrate strong potential for managing variable renewable resources. Advanced optimisation approaches including MILP based frequency stability constrained BESS sizing [18], multi time scale microgrid optimisation using BESS and HVAC (High Voltage Alternating Current) systems [19] and long term PV-BESS lifecycle cost modelling using MINLP [20] further highlight the importance of integrated renewable storage planning. However, these approaches remain designed for stationary microgrids and do not address outage-driven reliability or energy support for a moving high speed train.

Reliability analysis plays a foundational role in power system distribution planning [21], [22]. The distribution indices such as System Average Interruption Frequency Index (SAIFI), System Average Interruption Duration Index (SAIDI), Expected Energy Not Supplied (EENS) and Loss of Load Probability (LOLP) widely used to quantify service continuity [23], [24]. Analytical formulations for interruption duration and energy not supplied have been developed

Power System Technology
ISSN:1000-3673
Received: 16-11-2025 Revised: 05-12-2025 Accepted: 30-01-2026

for distribution systems [25] and renewable integration is shown to enhance reliability under uncertain operating conditions [26]. Additional research has examined generation adequacy [27], transmission link failures [28], and cyber physical vulnerabilities through insurance based reliability support [29, 30]. However, these studies do not capture operational characteristics of high speed electric railways. Bullet trains act as dynamic and mobile loads requiring uninterrupted traction power across sequential substations, making them highly susceptible to location specific grid disturbances. This necessitates a dedicated reliability evaluation framework tailored to outage driven railway energy behaviour.

Despite extensive progress in renewable integration, microgrid optimisation and reliability modelling, existing literature falls short when applied to high speed electrified railways. Most existing models assume continuous grid availability and therefore fail to assess traction power reliability along a moving train's journey under temporal grid failures. Minute-wise reliability indices such as EENS, SAIFI, SAIDI and LOLP have not been evaluated under outage conditions and the cost reliability trade-off associated with constrained PV-BESS sizing and outage-time energy dispatch remains unexplored. These limitations highlight the need for a unified framework that integrates outage modelling, renewable storage interaction, and cost reliability optimisation for resilient traction power support.

To address these gaps, this work develops a multi scenario optimisation framework to ensure reliable and cost effective energy management for high speed bullet trains under stochastic grid outage conditions. The proposed framework integrates PV generation, battery storage and substation support across three structured scenarios. Scenario 1 utilises Benders decomposition to model full journey having random load and noisy solar profiles. Further, Scenario 2 analyses the segment based reliability under realistic load and ideal solar profiles using Benders decomposition technique. Furthermore, Mixed integer linear programming (MILP) is employed in scenario 3 to implement a strategic planning that balances the trade-off between cost and reliability. Scenarios 1 and 2 enables minute-wise estimation of reliability indices and optimal PV-BESS sizing with associated investment costs. Scenario 3 quantifies the cost reliability trade-off by evaluating system performance under varying EENS thresholds and budget constraints. Together, these scenarios offer a unified, scalable approach to designing outage resilient renewable supported traction power systems for high speed railways.

The main contributions of this article are as follows:

(1) A multi scenario optimisation framework is developed to model stochastic grid outages with minute level temporal resolution, enabling detailed assessment of traction power continuity along entire high speed rail trajectory.

(2) Incorporated realistic stochastic load solar profiles to capture PV-BESS interaction dynamics and support adaptive sizing of renewable and storage assets under diverse outages.

Power System Technology
ISSN:1000-3673
Received: 16-11-2025 Revised: 05-12-2025 Accepted: 30-01-2026

(3) Designed a Benders decomposition structure in which the master problem determines optimal PV-battery sizing while the subproblem performs outage driven Monte Carlo simulation for reliability evaluation.

(4) A Mixed Integer Linear Programming (MILP) formulation is utilised to quantify the cost reliability trade-off under varying EENS thresholds and budget limits, providing actionable insight into investment requirements for reliability enhancement.

(5) Computed minute-wise reliability indices (EENS, SAIFI, SAIDI, LOLP) along the entire journey to identify outage sensitive intervals and guide power system planners in designing renewable supported traction power systems.

The remaining of this paper is organised as follows: Section 2 outlines the problem motivation and technical background for the research problem. Section 3 details the problem methodology including optimisation framework, reliability assessment procedure. Section 4 elaborately explains the simulation results validating the proposed work. Section 5 concludes the paper with crucial remarks of proposed work.

2. Problem Motivation

Figure 1: Energy management of bullet train

Bullet train project is a natural milestone in infrastructure resilience, and technological self reliance. However, operating high speed railways requires uninterrupted energy delivery especially under grid vulnerabilities. Nevertheless, high speed trains are characterised by sharp acceleration loads, cruising phases, and deceleration points, all requiring precisely coordinated energy support. Further, the grid failure makes the train stall causing service continuity and

Power System Technology
ISSN:1000-3673
Received: 16-11-2025 Revised: 05-12-2025 Accepted: 30-01-2026

passenger safety. Therefore, smart energy management strategy is much needed under grid outages by utilising substation supply, PV generation, battery storage support.

A smart energy management framework where the energy requirement of train across entire journey is estimated in advance under the potential grid failure. This pre-outage energy estimation will be served as input guides the energy planners about output energy dispatch during outage conditions. Once a grid outage occurs, the bullet train is supplied by utilizing the previously estimated energy demand from PV and battery systems. Moreover, the energy management framework ensures continual train operation by utilising substation, PV generation and battery storage during outage conditions. Further, the overall architecture shown in Figure 1 mimics a closed loop control system. The bullet train acting as a controlled plant and the trio of substation, battery, PV collectively act as a feedback mechanism. Furthermore, the closed loop energy management provides an adaptive energy management layer, ensuring reliability in real time railway energy systems.

Besides, financial resources are essential to ensure the estimation of energy support due to their costs associated with battery and PV sizing. Therefore, determining the optimal sizing and dispatch of these resources without excessive financial burden is essential to ensure reliable power delivery. The challenge lies in designing a strategy where reliability is improved, while over all energy support costs remain within acceptable limits. It is imperative to establish an optimal trade-off between economic cost and system reliability to ensure smart energy management in high speed rail energy planning.

3. Proposed Methodology

Three scenarios have been formulated to evaluate reliability of the bullet train's power system under grid outage conditions. These scenarios are designed to capture variations in grid failure timing, energy management providing a detailed assessment of reliability across the entire journey. The optimised battery and PV combinations along with their costs are estimated utilising Benders decomposition technique under Scenarios 1 and 2 respectively. Scenarios 1 defined as Stochastic based Benders reliability assessment and Scenario 2 known as Segment based Benders reliability assessment are evaluated under various load and solar uncertainty profiles. The methodology of both scenarios 1 and 2 are explicitly explained below.

3.1 Modelling of Scenarios 1 and 2 under Benders Decomposition Framework

Step 1: Initialise the indices, parameters and decision variables required for solving the benders decomposition optimisation problem.

- $t = \{1, 2, 3 \ldots\ldots, T\}$ represents the time index in minutes
- $\Phi \subset t$, where Φ represents the starting outage of the minute
- $m = 1, \ldots\ldots, M$ represents the Monte Carlo simulation index

Power System Technology
ISSN:1000-3673
Received: 16-11-2025 Revised: 05-12-2025 Accepted: 30-01-2026

- k : Benders iteration index
- $\mathbb{Z}(t)$: Train load demanded at time t in MW
- β : EENS threshold limit in MWh
- $\mathbb{C}_b$: cost per MWh battery in crores
- $\mathbb{C}_p$: cost per MW solar PV in crores
- Υ_b : Battery capacity in MWh
- Υ_p : PV capacity in MW

Step 2: The generalised procedure for modelling the load profile, grid outage, PV generation, battery storage and energy support have been explained in the following steps. Here, the impact on reliability indices resulting from energy dispatch and power delivery during grid outage conditions is examined using the Benders decomposition approach. This approach facilitates the assessment of how optimally sized PV and battery systems respond to outages, highlighting their effectiveness in maintaining service continuity throughout bullet train journey.

Step 2(a): In Scenario 1, the train load is modelled using a uniformly distributed random variable (Γ) bounded between minimum load ($\mathbb{Z}_{min}$) and maximum load ($\mathbb{Z}_{max}$) values at respective $'t'$ duration time index.

$$\mathbb{Z}(t) = \mathbb{Z}_{\min}(t) + (\mathbb{Z}_{\max}(t) - \mathbb{Z}_{\min}(t)).\Gamma \quad (1)$$

The total train load over a 120 minute journey is interpreted as a union of 12 identical segment level load profiles, each lasting 10 minutes. Further, the Scenario 2 load profile (L(t)) having acceleration, cruise and deceleration phases are shown in equation (2). Here, σ differentiates the various phases of train journey in the considered segment. Here t_1, t_2, t_3 corresponds to 2, 8, 10 minutes and the same procedure is iteratively applied over successive time intervals until the entire journey duration is covered.

$$L(t) = \begin{cases} 5\sigma, & 0 \le \sigma < t_1 \\ 10, & t_1 \le \sigma < t_2 \\ max(0.5, 10 - 4.75(\sigma - 8)), & t_2 \le \sigma < t_3 \end{cases} \quad (2)$$

Step 2(b): In Scenario 1, the PV generation profile ($\mathbb{P}_t^p$) is modelled with randomised noise (λ) to reflect natural variability shown mathematically in equation (3). Similarly, the PV generation profile ($\mathbb{P}_t^{p\prime}$) under Scenario 2 is defined in equation (4) and randomised noise (λ) is not considered here. Equation (5) depicts the idealised solar generation profile, follows the sinusoidal pattern that reaches its maximum at midpoint of journey in Scenario 2. This approach captures the natural solar irradiance pattern, assuming maximum irradiance at mid duration. Similarly, a randomised solar profileis considered in Scenario 1, where ψ is the randomised noise in equation (6). Further, different solar profiles allows the Benders decomposition to test how PV and battery systems under multi uncertainty conditions. The PV

Power System Technology
ISSN:1000-3673
Received: 16-11-2025 Revised: 05-12-2025 Accepted: 30-01-2026

capacity corresponding to outage time is denoted by Υ_p^{Φ} and determined using the Benders decomposition framework. This capacity reflects the optimal PV sizing required to maintain system reliability during the outage periods (Φ).

$$\mathbb{P}_t^p = min(\Upsilon_p^{\Phi}, max(0, \Upsilon_p^{\Phi}.\mu_t + \lambda)) \quad (3)$$

$$\mathbb{P}_t^{p\prime} = min(\Upsilon_p^{\Phi}, max(0, \Upsilon_p^{\Phi}.\mu_t)) \quad (4)$$

$$\mu_t = sin\left(\frac{\pi t}{T}\right) \quad (5)$$

$$\mu_t' = sin\left(\frac{\pi t}{T}\right) + \psi \quad (6)$$

Step 2(c): The battery power contributions i.e. $\mathbb{P}_t^b$ for Scenatio 1 and $\mathbb{P}_t^{b\prime}$ for Scenario 2, during grid outage conditions are modelled using equations (7) and (8) respectively. These equations capture the battery's role in maintaining train load under grid outages. Additionally, the dispatch formulations are designed to quantify the battery's support only after the available PV supply has been fully utilized. In this energy dispatch model, the battery is activated to compensate for the deficit energy only when the PV generation is insuffcient to meet the train's load demand. The battery contribution corresponding to outage time is denoted by Υ_b^{Φ} and it is obtained using the Benders decomposition framework.

$$\mathbb{P}_t^b = min(\Upsilon_b^{\Phi}, \mathbb{Z}(t) - \mathbb{P}_t^p) \quad (7)$$

$$\mathbb{P}_t^{b\prime} = min(\Upsilon_b^{\Phi}, \mathbb{Z}(t) - \mathbb{P}_t^{p\prime}) \quad (8)$$

Step 2(d): The binary status of grid ($S_g^i(t)$) depends on normal and outage conditions. During normal condition, the train load demand ($\mathbb{Z}(t)$) is supplied through substations. While under outage conditions, the load is supported by battery and PV systems. Further, equation (9) showcases the demand met (D(t)) under grid working and failure conditions of scenario 1 respectively. Similarly, equation (9) is valid for Scenario 2 where $\mathbb{P}_t^p, \mathbb{P}_t^b$ are replaced with $\mathbb{P}_t^{p\prime}, \mathbb{P}_t^{b\prime}$ and the load profile $\mathbb{Z}(t)$ with L(t).

$$\mathrm{D(t)} = \begin{cases} \mathbb{Z}(t), & S_g^i(t) = 1 \\ min(\mathbb{Z}(t), \mathbb{P}_t^p + \mathbb{P}_t^b), & S_g^i(t) = 0 \end{cases} \quad (9)$$

Step 3: The Benders optimisation framework is employed to determine the optimal battery and PV sizing by simulating specific outage duration. Further, minimising over all cost (J) is the primary objective of Benders master problem as shown in equation (10). Moreover, equations (11) and (12) represents the EENS (expected energy not supplied) threshold limit and Benders cut constraints (ϱ_{cuts}) which are utilised in guiding the master problem. Thus, equations (10), (11), (12) ensure that optimization framework maintains the reliability requirements while achieving cost efficient PV and battery sizing. Additionally, equations (13) and (14) specify

Power System Technology
ISSN:1000-3673
Received: 16-11-2025 Revised: 05-12-2025 Accepted: 30-01-2026

that power output from PV and battery system must remain within their respective maximum rated capacities.

$$minimize \ \{J = \Upsilon_p^{\Phi}.\mathbb{C}_p + \Upsilon_b^{\Phi}.\mathbb{C}_b\} \tag{10}$$

Subject to:

$$EENS\,(\Upsilon_p^{\Phi}, \Upsilon_b^{\Phi}) \leq \beta \tag{11}$$

$$\Upsilon_p^{\Phi}, \Upsilon_b^{\Phi} \notin \varrho_{cuts} \tag{12}$$

$$0 \leq \Upsilon_p^{\Phi} \leq \Upsilon_p \tag{13}$$

$$0 \leq \Upsilon_b^{\Phi} \leq \Upsilon_b \tag{14}$$

Step 4: The battery and PV sizing determined from master problem are subjected to Monte Carlo simulation (MCS) with N trials. Then, the reliability indices are estimated in the sub level problem. Further, this analysis captures the variability in solar generation and load profiles during simulated outage scenarios. Furthermore, the scenarios containing time varying outages, repeated reliability estimation, and separable dispatch logic are best handled by Benders Decomposition.

$$EENS^{(i)} = \sum_{t=\Phi}^{T} \left[\mathbb{Z}\,(t)^{(i)} - D(t)^{(i)}\right].\Delta t \tag{15}$$

$$EENS^{(k)} = \frac{1}{N}\sum_{i=1}^{N} EENS^{(i)} \tag{16}$$

$$\mathbb{M}^{(i)} = \mathbb{A}\left[\mathbb{Z}\,(t)^{(i)} > P_t^{del(i)}\right] \tag{17}$$

$$SAIFI^{(i)} = \sum_{t=\Phi}^{T} \mathbb{M}_t^{(i)} \tag{18}$$

$$SAIFI^{(k)} = \frac{1}{N}\sum_{i=1}^{N} SAIFI^{(i)} \tag{19}$$

$$SAIDI^{(i)} = \sum_{t=\Phi}^{T} \mathbb{Y}_t^{(i)} \tag{20}$$

$$SAIDI^{(k)} = \frac{1}{N}\sum_{i=1}^{N} SAIDI^{(i)} \tag{21}$$

Power System Technology
ISSN:1000-3673
Received: 16-11-2025 Revised: 05-12-2025 Accepted: 30-01-2026

$$LOLP^{(i)} = \frac{SAIDI^{(i)}}{Duration} \tag{22}$$

$$LOLP^{(k)} = \frac{1}{N}\sum_{i=1}^{N} \frac{SAIDI^{(i)}}{Duration} \tag{23}$$

The expected energy not supplied (EENS) for each trial $'i'$ starting from a specified outage time ($'\Phi'$) is shown in equation (15). Subsequently, the MCS is performed ovr trials to compute the mean EENS as shown in equation (16). Besides, equation (17) counts the power demand unmet by PV and battery systems during trial $'i'$. Thus, these interruptions tends to evaluate system average interruption frequency index (SAIFI) using MCS from equations (18) and (19) respectively. Here, $P_t^{del(i)}$ is the combined power delivered by battery and PV for trial $'i'$. Further, $\mathbb{Y}_t^{(i)}$ represents the duration of power demand unmet by PV and battery systems. The system average interruption duration index (SAIDI) represents the total duration of unmet demand is estimated by using equations (20) and (21). Consequently, loss of load probability (LOLP) which is a characteristic property of SAIDI is computed using equations (22) and (23). Further, this iterative procedure has been continued until the condition $EENS^{(k)} \leq \beta$ is satisfied. If the condition is not met, a new Benders cut is added and then the master problem is re-optimised to estimate the optimal battery and PV sizing. Similar computational procedure has been performed for Scenario 2 to estimate reliability indices, however load profile $\mathbb{Z}(t)$ is replaced with L(t).

Step 5: Thus, the following outcomes are evaluated under outage time simulation are as follows:

- Optimal sizing of PV and battery systems
- Reliability indices i.e. EENS, SAIFI, SAIDI, LOLP
- Total cost estimation

3.2. Modelling of Scenario 3 under MILP Framework

Scenario 3, a joint cost MILP reliability formulation aims to achieve a cost effective and reliable energy support system by coordinating optimal sizing of battery and PV resources. Further, this scenario ensures that reliability is maintained through out the journey while satisfying both cost and EENS constraints. Furthermore, a fixed outage is modelled determine istically for analysis. Besides, this study investigates cost constrained optimization focused on minimizing EENS within predefined financial limits. Conversely, a reliability constrained optimization is examined to minimize the overall cost ensuring that EENS remains within specified reliability limits. Scenarios where outage conditions are fixed and joint cost reliability trade-off is modelled as a single problem are efficiently handled by MILP.

Power System Technology
ISSN:1000-3673
Received: 16-11-2025 Revised: 05-12-2025 Accepted: 30-01-2026

Step 1: Initialise the indices, parameters and decision variables essential for solving the MILP problem.

- Load profile L(t) in MW for each minute t
- Outage status ξ indicating a fixed deterministic outage occurrence
- Battery charging and discharging efficiencies: η_{ch}, η_{dis}
- Time resolution: $\Delta t = 1\, minute = \frac{1}{60}\, hours$
- $\mathbb{G}_p(t)$: PV power supplied to load at time t
- $\mathbb{G}_b(t)$: Battery power supplied to load at time t
- $P_u(t)$: Excess PV power stored into battery
- $\mathbb{B}(t)$: Battery state of charge
- $E_{eens}(t)$: Unserved load during outage
- Θ_p : Total PV capacity installed
- Θ_b : Total battery capacity installed

Step 2: A strategic joint cost reliability optimisation framework is implemented to assess reliability of bullet train power system using MILP. Further, MILP based cost constrained optimisation is solved for different target EENS levels shown in equations (24) and (25). Furthermore, MILP based EENS constrained optimisation is solved for different target cost levels shown in equations (26) and (27). Equations (25) and (27) represents the constraints of cost and EENS limits. The PV capacity (Θ_p^{ξ}) and battery contribution (Θ_b^{ξ}) corresponding to blackout occurrence are determined through MILP.

$$minimize\left\{\sum_{t=1}^{T} E_{eens}(t)\right\} \tag{24}$$

$$\Theta_p^{\xi}\mathbb{C}_p + \Theta_b^{\xi}\mathbb{C}_b \leq Budget\ Limit \tag{25}$$

$$minimize\left\{\Theta_p^{\xi}\mathbb{C}_p + \Theta_b^{\xi}\mathbb{C}_b\right\} \tag{26}$$

$$\sum_{t=1}^{T} E_{eens}(t) \leq EENS\ Limit \tag{27}$$

Step 3: Equation (28) represents the power balance relationship during grid outage conditions. It ensures that sum of power supplied by battery and PV matches the train's load demand, with any shortfall represented as unserved energy. Equation (29) illustrate the battery state of charge dynamics with charging and discharging constraints. Additionally, equations (30) and (31) specify that power output from PV and battery system must remain within their respective maximum rated capacities.

Power System Technology
ISSN:1000-3673
Received: 16-11-2025 Revised: 05-12-2025 Accepted: 30-01-2026

$$\mathbb{G}_p(t) + \mathbb{G}_b(t) + E_{eens}(t) = \mathrm{L(t)} \quad (28)$$

$$\mathbb{B}(t) = \mathbb{B}(t-1) + \eta_{ch} P_u (t-1)\Delta t - \frac{P_{batt}(t-1)\Delta t}{\eta_{dis}} \quad (29)$$

$$0 \leq \Theta_p^{\xi} \leq \Theta_p \quad (30)$$

$$0 \leq \Theta_b^{\xi} \leq \Theta_b \quad (31)$$

Step 4: The simulation under outage conditions is carried through MILP, solved by using intlingprog function for the following cases.

Step 4(a):

- Solve joint cost reliability optimisation
- Estimate the energy and power supported by PV and battery systems

Step 4(b):

- Solve cost constrained optimisation
- Estimate the reliability indices

Step 4(c):

- Solve EENS constrained optimisation
- Estimate the total cost

Figure 2 illustrates the computational procedure and methodology of work which is represented in a flow chart for visualisation.

Power System Technology
ISSN:1000-3673
Received: 16-11-2025 Revised: 05-12-2025 Accepted: 30-01-2026

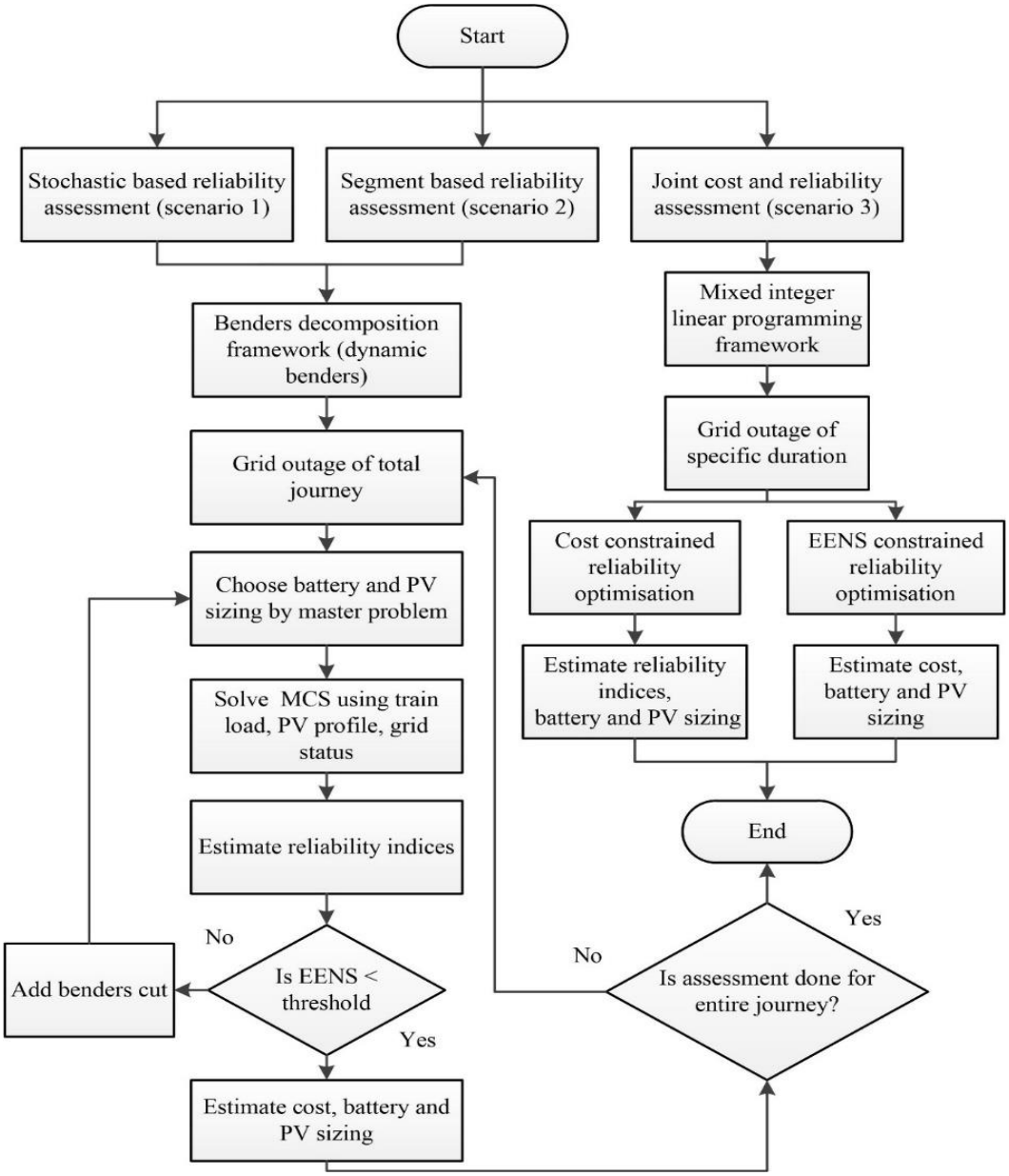

Figure 2: A flowowchart illustrating the computational procedure

4. Simulation Results

The high speed electrified bullet train under multi uncertainty dynamic scenarios are analysed by the Benders decomposition and MILP optimisation techniques. Further, three scenarios are classified to validate the proposed methodology in the simulation results. Scenario 1 capturers the characteristics namely reliability indices, power delivery, optimised battery and PV sizing along with their costs across randomised load and solar profile over the entire journey duration.

Power System Technology
ISSN:1000-3673
Received: 16-11-2025 Revised: 05-12-2025 Accepted: 30-01-2026

Scenario 2 capturers the identical characteristics of the scenario 1 but, the segment wise based train load and ideal solar profile are utilised. Scenario 3 focusses joint cost MILP strategic framework which is implemented to explore optimal cost reliability compliance. The costs associated with 1 MWh battery and 1 MW solar PV are 2.5 and 8 crores respectively.

Table 1: Scenario 1 Reliability Indices

Reliability Paramerters	Case 1(a)	Case 1(b)	Case 1(c)	Case 1(d)	Improvement (%)
EENS (MWh)	0.1710	0.0000	0.5631	0.0059	98.95
SAIFI (Int)	1.3500	0.2200	0.5700	0.4300	24.56
SAIDI (min)	1.3500	0.2200	5.1600	0.4800	90.75
LOLP	0.0112	0.0018	0.0430	0.0040	90.69
Cost (crores)	0	33	33	36	9.09

4.1. Scenario 1: Stochastic based Benders Reliability Assessment

Scenario 1 represents the bullet train reliability analysis of a full journey using Benders decomposition under randomised load and noisy solar proles. Besides, Scenario 1 is characterised into four sub cases i.e. case 1(a), 1(b), 1(c), 1(d). Further, case 1(a) indicates the base case reliability under 1% grid outage in a 120 minute journey i.e. grid support. This case 1(a) is utilised to evaluate base line reliability under normal grid support. In addition, it helps to quantify the reliability indices without renewable supply. Furthermore, case 1(b) constitutes the optimal battery and PV sizing obtained from Benders decomposition under 10% grid outage. This case 1(b) considered as optimised Benders signifies the renewable support to maintain the reliability. Moreover, case 1(b) aims to minimise total cost investment by achieving optimal battery and PV combination with considering EENS as constraint.

Here, case 1(c) i.e. (optimised Benders minute-wise) inspects the outage at every minute in a full journey of a train. It estimates the reliability indices by utilising a fixed battery and PV combination obtained from case 1(b). Thus, this case will be useful for testing the battery and solar penetration under time varying outage scenarios. Finally, case 1(d) assess the reliability of bullet train system under blackout period by implementing a dynamic Benders decomposition technique. Unlike case 1(c), dynamic Benders (case 1(d)) designs an adaptive battery and PV sizing which performs re-optimisation at every black out minute. Besides, case 1(d) provides an estimate of necessary battery and PV sizing for effective energy management planning by power system energy planners under blackout periods. The improvement column

Power System Technology
ISSN:1000-3673
Received: 16-11-2025 Revised: 05-12-2025 Accepted: 30-01-2026

in the Table 1 reflects the performance gain of Case 1(d)'s dynamic, outage adaptive Benders optimisation compared with Case 1(c)'s fixed optimised Benders (minute-wise) sizing.

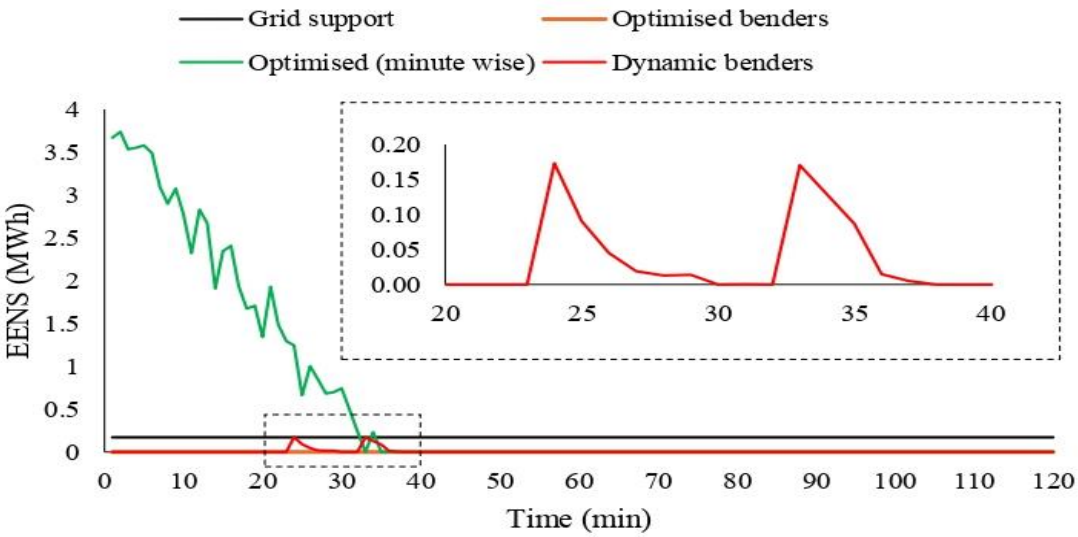

Figure 3: Minute-wise variation of EENS under Scenario 1

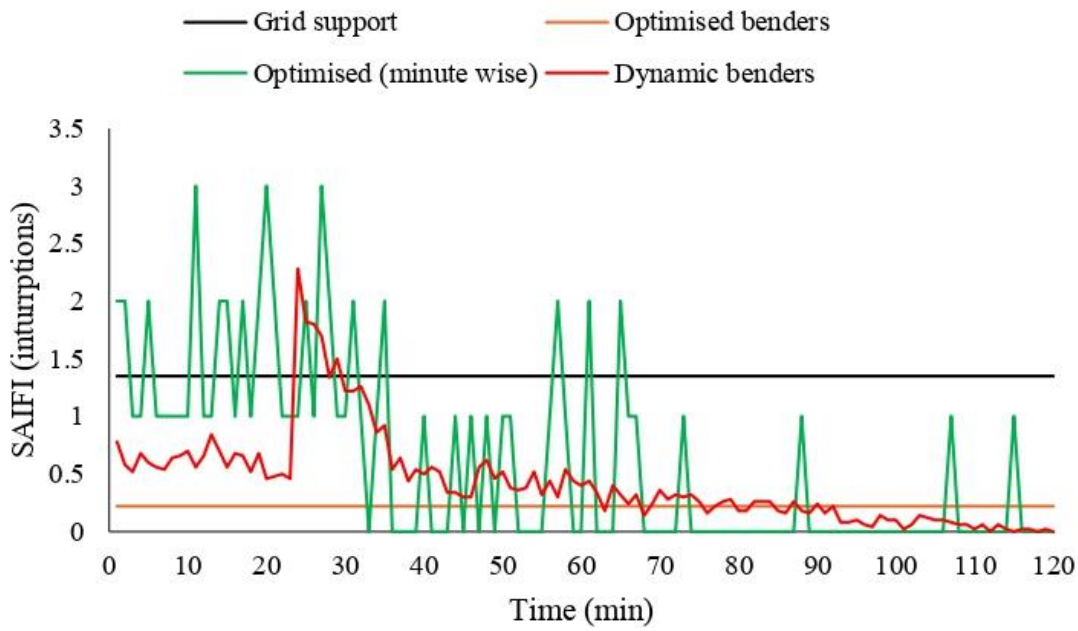

Figure 4: Minute-wise variation of SAIFI under Scenario 1

Power System Technology
ISSN:1000-3673
Received: 16-11-2025 Revised: 05-12-2025 Accepted: 30-01-2026

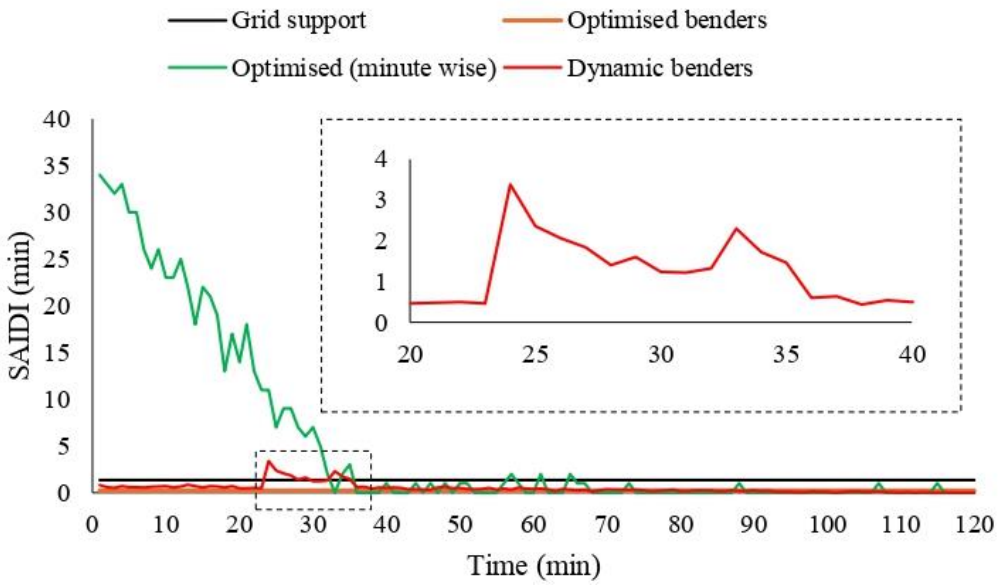

Figure 5: Minute-wise variation of SAIDI under Scenario 1

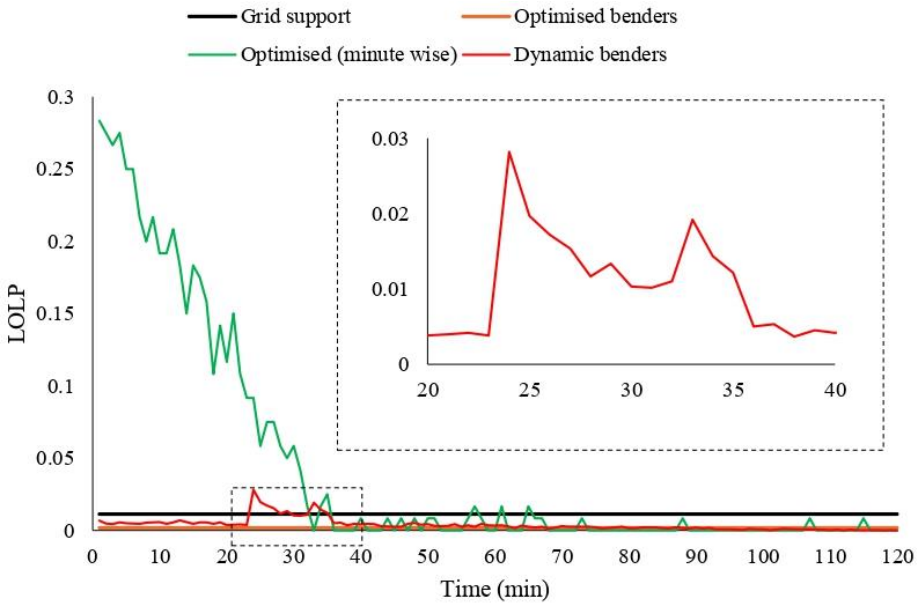

Figure 6: Minute-wise variation of LOLP under Scenario 1

Figures 3, 4, 5, 6 represents the minute-wise variation of reliability indices by using the cases 1(a), 1(b), 1(c), 1(d) under Scenario 1 respectively. It is found that the reliability indices of cases 1(a), 1(b) are having constant straight line characteristics as the grid outage is fixed (1% and 10%). Here, the simulation set up does not dependant on outage timing under the cases 1(a) and 1(b). The mean reliability indices namely EENS, SAIFI, SAIDI, LOLP of cases 1(a), 1(b) are 0.1710, 1.3500, 1.3500, 0.0012 and 0.000, 0.2200, 0.2200, 0.0018 respectively as

Power System Technology
ISSN:1000-3673
Received: 16-11-2025 Revised: 05-12-2025 Accepted: 30-01-2026

shown in Table 1. It is observed that there has been a drastic improvement in reliability indices under case 1(b). The 10 MWh battery and 1 MW PV combination obtained from Benders decomposition method is the reason for this improvement under case 1(b). But, this obtained optimal combination does not guarantee the reliability as it is simulated under static timing i.e. 10% grid outage. Therefore, case 1(c) estimates the reliability indices under full journey with optimum PV and battery combination obtained from case 1(b).

Figure 3 illustrates the minute wise comparison of EENS under Scenario 1. It is observed that during the initial time of journey, the EENS was 3.671 MWh and then EENS was dropped to zero at 36 minutes under case 1(c) respectively as shown in green colour. The high EENS observed during the early stages of the journey is due to the increased burden on the limited 1 MW PV system and 10 MWh battery configuration, following grid failure. Further, a grid failure at 20^{th} minute is more vulnerable compared to 70^{th} minute of journey. This is because the former case requires battery and PV system to support remaining 100 minutes of journey, but where as in latter case, the energy support is required for 50 minutes respectively. Further, similar observation has been valid for SAIDI and LOLP having initial interruption of 34 minutes per trip and 3.67% respectively during journey of first minute. Interestingly, Figures 5 and 6 represents the identical characteristics of SAIDI and LOLP. Here, LOLP, a ratio of SAIDI to the total journey duration is main reason for identical characteristics. Figure 4 represents multiple discrete interruptions represented by spikes. Generally, SAIFI is dependant on number of service interruptions whenever load cannot be fully met.

An one size fit optimal PV and battery combination utilised in case 1(c) does not suit for time varying sensitivity outages and therefore case 1(d) i.e. dynamic Benders is evaluated. The mean EENS, SAIFI, SAIDI, LOLP of case 1(d) were 0.0059, 0.4300, 0.4800, 0.0040 respectively and are improved values compared to other cases as shown in Table 1. Upon observing Figure 5, the SAIDI values for cases 1(c) and 1(d) at 19^{th} minute of journey were 17 and 0.68 minutes respectively, indicating a signifcant improvement in service continuity in case 1(d). Dynamic Benders re optimizes PV-battery sizing at every outage instant, unlike the static sizing in case 1(c). Thus dynamic Benders adaptive strategy achieves a 98.95%, 24.56%, 9.75%, 90.69% reduction in EENS, SAIFI, SAIDI, LOLP respectively as shown in Table 1. These improvements are achieved with a modest increase in cost, reflecting the enhanced reliability provided by the dynamic Benders optimisation. Further, adaptive battery and PV sizing estimation at specific outage minute by the dynamic Benders demonstrate the time varying sensitivity outage planning. Thus, the dynamic Benders optimisation estimates the proper battery and PV backup required for continuous operation of bullet train.

Power System Technology
ISSN:1000-3673
Received: 16-11-2025 Revised: 05-12-2025 Accepted: 30-01-2026

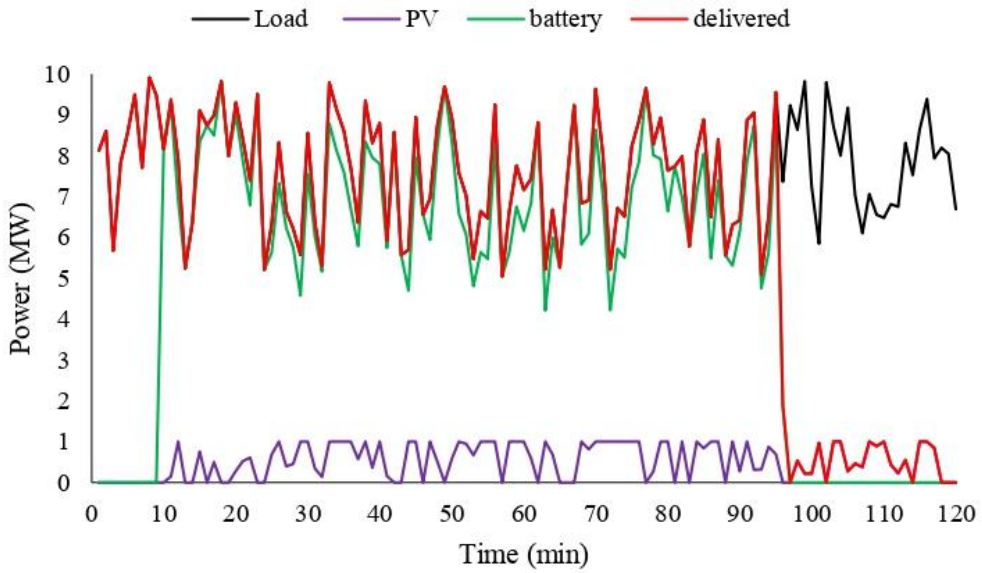

Figure 7: Power delivered by optimised Benders at t = 10th minute outage under Scenario 1

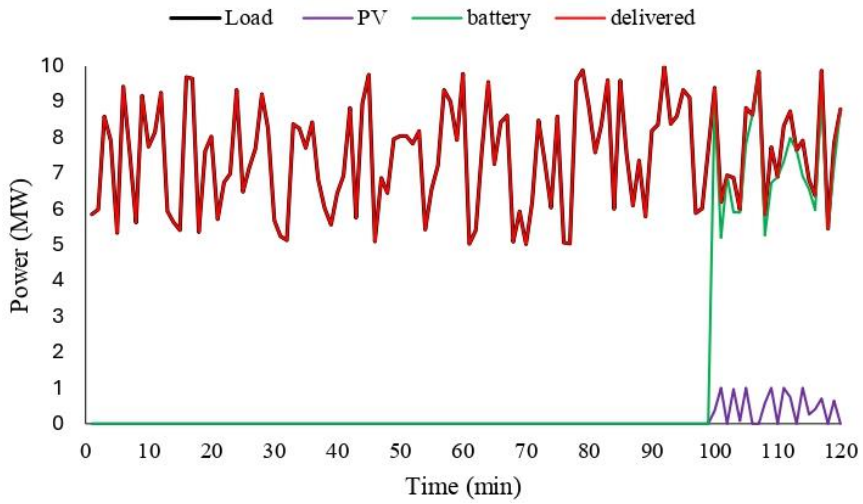

Figure 8: Power delivered by optimised Benders at t =100th minute outage under Scenario 1

Figures 7 and 8 illustrates the battery and PV power contributions by minute-wise optimised Benders (case 1(c)) during outages occurring at 10th and 100th minute respectively. The black, red, violet and green colours representing the train load, total power delivered to train, total power contributed by PV and battery respectively. It is revealed that the train load has been supplied from 10th minute to 98th minute with battery and PV support as shown in Figure 7. However, after the 98th minute the battery gets depleted and partial support is provided by PV causing interruptions and reduced service reliability. Figure 8 highlights total power contributed by battery and PV at 100th minute outage occurrence. The optimally sized battery and PV system are suffcient to meet demand as the grid support is upto 99 minutes.

Power System Technology
ISSN:1000-3673
Received: 16-11-2025 Revised: 05-12-2025 Accepted: 30-01-2026

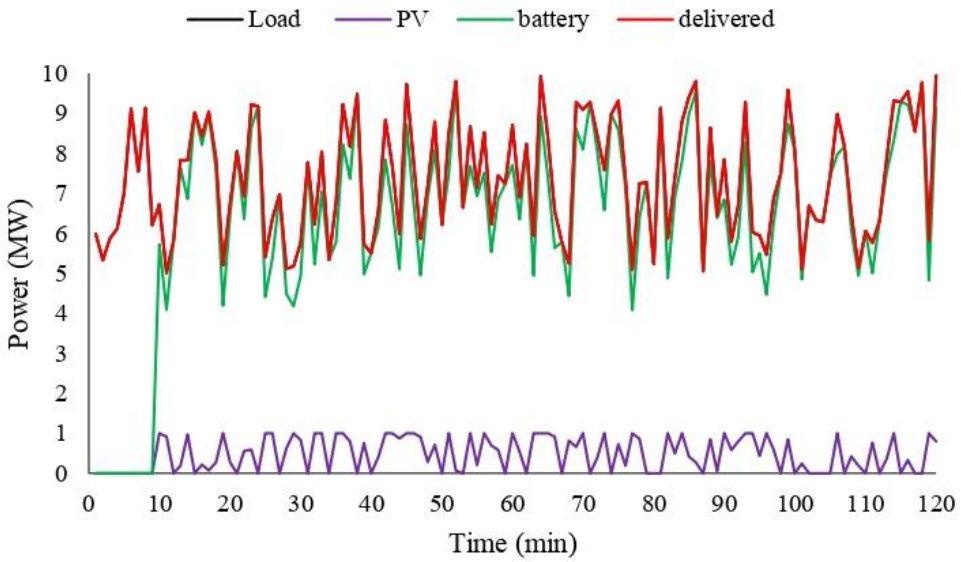

Figure 9: Power delivered by dynamic Benders at t = 10th minute outage under Scenario 1

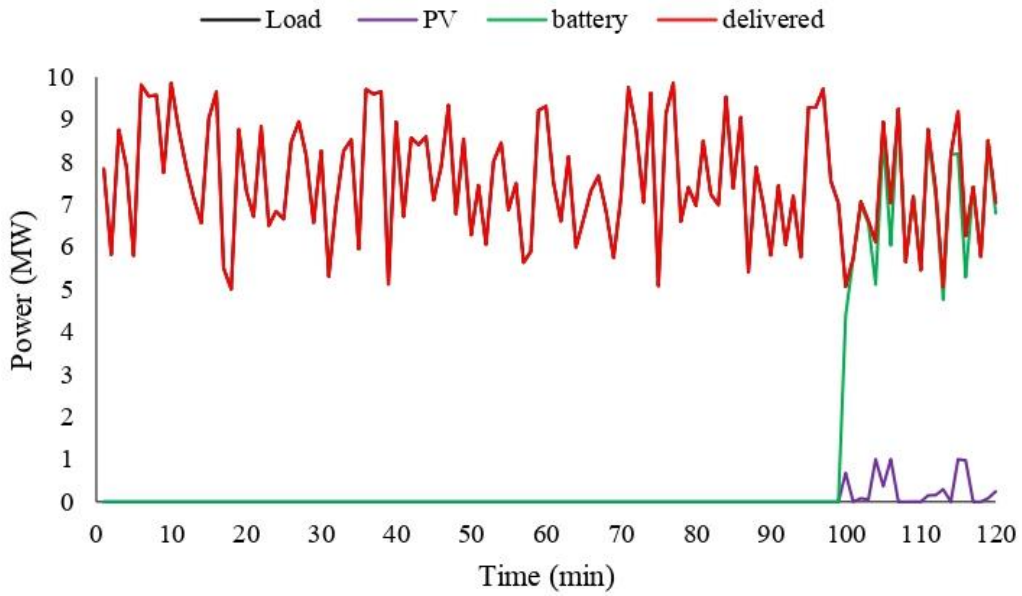

Figure 10: Power delivered by dynamic Benders at t = 100th minute outage under Scenario 1

Similarly, Figures 9 and 10 illustrates the battery and PV power contributions by dynamic Benders (case 1(d)) during outages occurring at 10th and 100th minute respectively. Interestingly, it is observed that total power has been delivered under both outage occurrences at 10th and 100th minute. The dynamic Benders approach estimates the optimal battery and PV system for each outage minute enables effective power delivery. Further, the selection of battery and PV configuration under every minute of journey guide the energy planners about dispatching the energy during sudden outage occurrences.

Power System Technology
ISSN:1000-3673
Received: 16-11-2025 Revised: 05-12-2025 Accepted: 30-01-2026

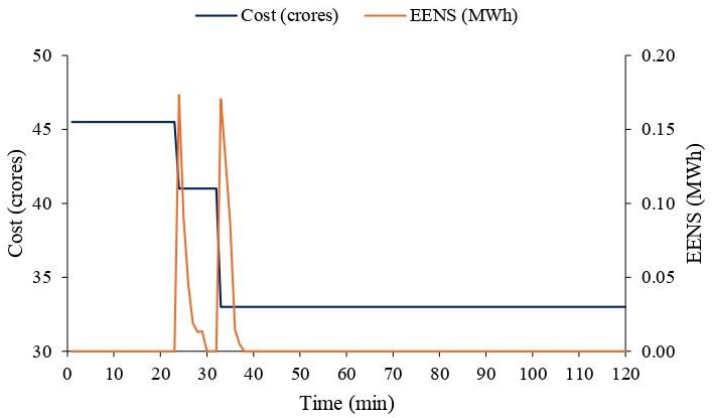

Figure 11: Cost and EENS trade off by dynamic Benders under Scenario 1

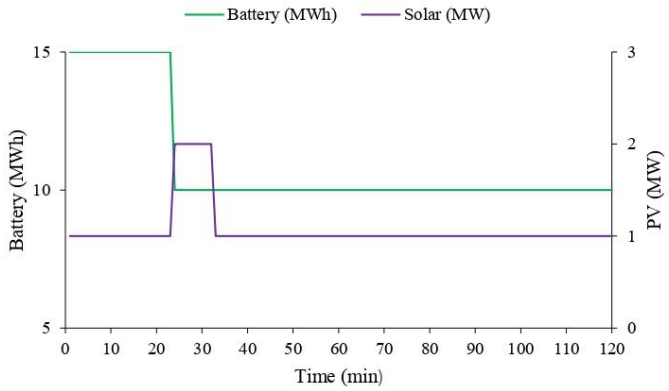

Figure 12: Battery and PV sizing by dynamic Benders under Scenario 1

Figure 11 illustrates the trade-off between cost and EENS when the outage is varying from 1 to 120 minutes of a full journey. It is revealed that an outage occurring within the first 20 outage minutes incurs a cost of 45 crores. The cost emphasizes the capital investment required for deploying battery and PV to ensure uninterrupted power supply during early stage interruptions. But, the interesting fact is that observed EENS is below 0.02 MWh threshold limit. Further, the total cost associated between outages starting from the 33rd to 120th minute was 33 crores under 0.2 MWh EENS threshold limit. It demonstrates that the obtained fixed back up system and their costs are sufficient for maintaining the reliability under grid failure conditions. A cost reliability trade-off demands a master level strategy to optimally size PV and battery systems under outage conditions. Thus, Benders decomposition enables this by separating sizing decisions from real time dispatch evaluation. Without Benders, bi-level optimization cannot be efficiently handled especially under time varying grid outages.

Figure 12 illustrates the optimal battery and PV sizing determined through dynamic Benders decomposition under outage period. During the initial outage period from the 1st to the 23rd minute, the battery and PV requirement were 15 MWh and 1 MW respectively. But from 23rd

Power System Technology
ISSN:1000-3673
Received: 16-11-2025 Revised: 05-12-2025 Accepted: 30-01-2026

minute, the PV generation is increased to 2 MW thereby reducing the battery capacity to 10 MWh. Thus, battery and PV contribution and their coordination obtained from dynamic benders aid in designing the energy dispatch strategy under blackout period. Due to the dynamic nature of outage timing, different dispatch strategies have to followed throughout the journey. Benders decomposition addresses this by solving dispatch sub problems for each outage instance to obtain PV and battery sizes to maintain reliability.

The main advantage of dynamic Benders (case 1 (d)) under Scenario 1 has been explained with an example. If a bullet train loses power at t^{th} minute, the master problem evaluates the battery and PV requirement for supporting energy from tth minute to remaining complete journey. Then, the sub problem decides the energy dispatch required under uncertain solar and load proles using Monte Carlo simulation (MCS). Finally, bi-level optimisation framework ensures optimal PV and battery sizing while minimizing overall system cost and enhancing reliability. Thus, the proposed method is well suited for energy management of high speed rail corridor.

4.2. Scenario 2: Segment based Benders Reliability Assessment

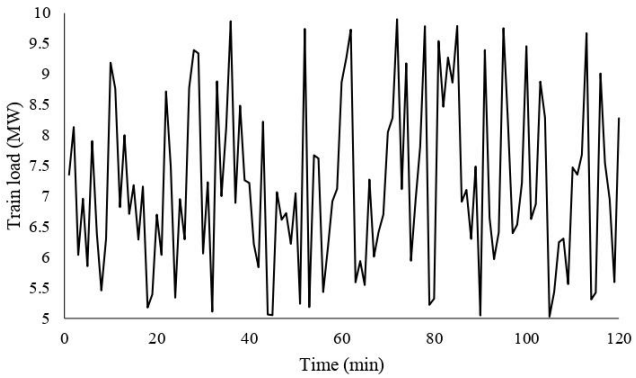

Figure 13: Train load profile for Scenario 1

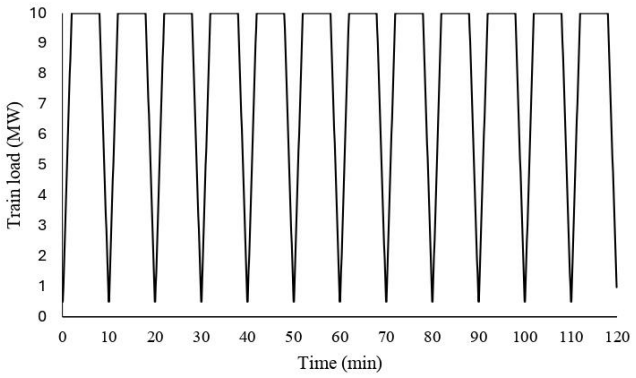

Figure 14: Train load profile for Scenario 2

Figure 13 represents the randomised train load profile for Scenario 1, Figure 14 represents segmented train load profile for Scenario 2 respectively. A 120 minute train journey load

Power System Technology
ISSN:1000-3673
Received: 16-11-2025 Revised: 05-12-2025 Accepted: 30-01-2026

profile is structured to capture dynamics of acceleration, cruise, deceleration phases shown in Figure 14. The journey is segmented into 12 equal parts having each inter station interval of 10 minutes. The acceleration phase (0-2) minutes features a linear increase in load from 0.5 MW to 10 MW. Further, the cruise phase (3-8) minutes having a constant 10 MW load and finally reduced to 0.5 MW in deceleration phase (9-10) minutes.

Here, case 2(a) represents the base reliability under 1% grid outage in a 120 minute journey. Further, case 2(b) indicates the optimal battery and PV combination obtained from Benders decomposition under 10% grid outage. Furthermore, case 2(c) (optimised Benders minute-wise) estimates the reliability of outage at every minute of journey utilising PV and battery capacity from case 2(b). Finally, case 2(d) estimates the optimum battery and PV by utilising dynamic Benders with re optimising every minute. Here, cases 2(a), 2(b), 2(c), 2(d) in scenario 2 are similar to cases 1(a), 1(b), 1(c), 1(d) in Scenario 1 respectively. But, the Scenarios 1 and 2 varies in train load and solar profile models respectively.

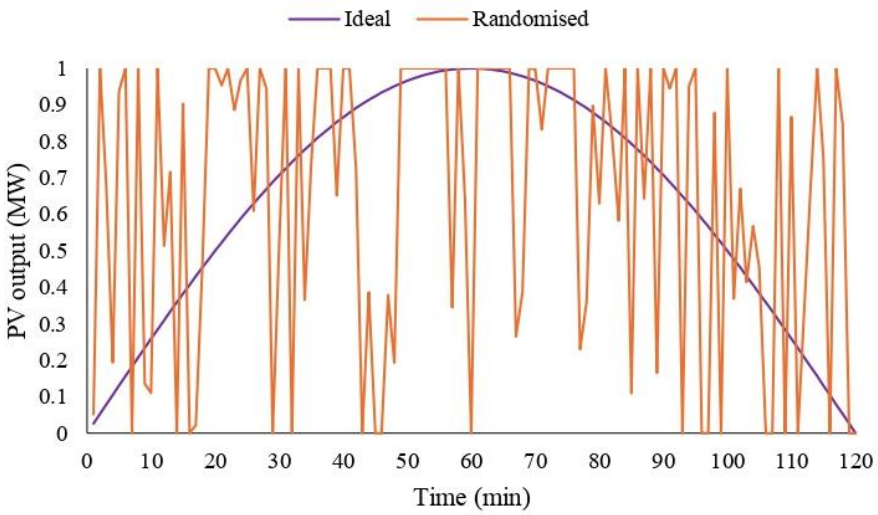

Figure 15: PV characteristics

To reflect realistic operational conditions, the bullet train's load profile is modelled as time varying. The power demand varies with acceleration, cruising, and deceleration. Therefore, a segment wise load profile shown in Figure 14 is employed to represent different phases of train operation such as start, run and stop conditions. A randomized load profile is considered to capture variations during continuous running conditions as shown in Figure 13. Further, a randomised solar PV profile for Scenario 1 and ideal solar PV profile for Scenario 2 are considered as shown in Figure 15. The improvement column in the Table 2 reflects the performance gain of Case 2(d)'s dynamic, outage adaptive Benders optimisation compared with Case 2 (c)'s fixed optimised Benders (minute-wise) sizing.

Power System Technology
ISSN:1000-3673
Received: 16-11-2025 Revised: 05-12-2025 Accepted: 30-01-2026

Table 2: Scenario 2 Reliability Indices

Reliability Paramerters	Case 2(a)	Case 2(b)	Case 2(c)	Case 2(d)	Improvement (%)
EENS (MWh)	0.1663	0.00	4.2913	0.0150	99.65
SAIFI (Int)	1.2500	0.00	1.0200	0.5900	42.15
SAIDI (min)	1.3500	0.00	43.2100	0.8110	98.12
LOLP	0.0104	0.00	0.3600	0.0067	98.13
Cost (crores)	0	21	21	33	59.28

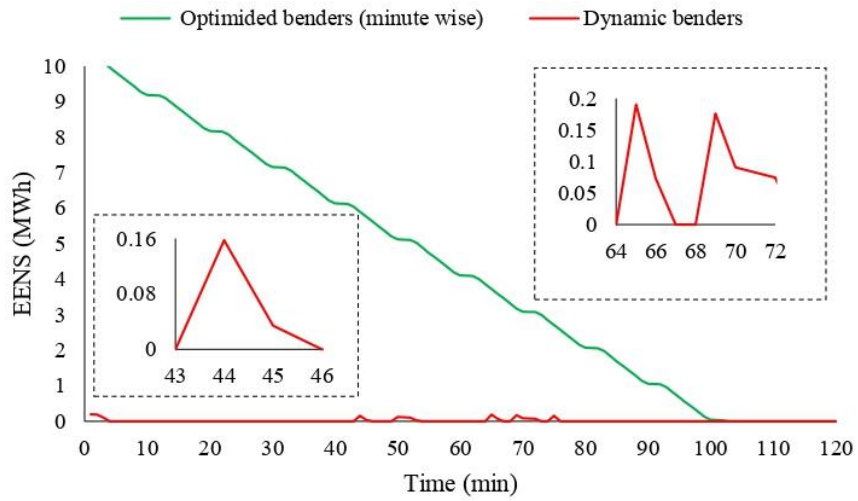

Figure 16: Minute-wise variation of EENS under cases 2(c) and 2(d)

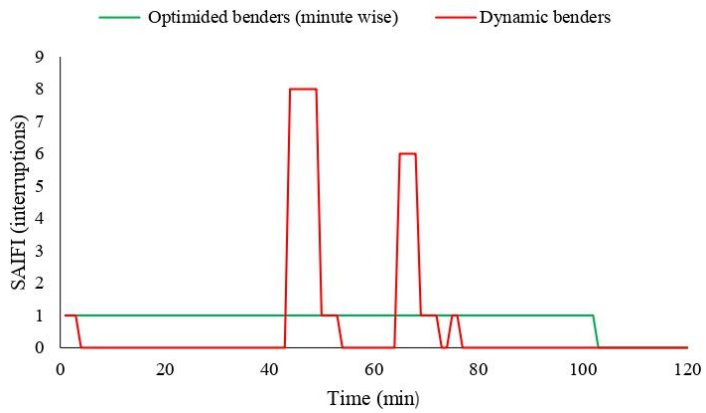

Figure 17: Minute-wise variation of SAIFI under case 2(c) and 2(d)

Power System Technology
ISSN:1000-3673
Received: 16-11-2025 Revised: 05-12-2025 Accepted: 30-01-2026

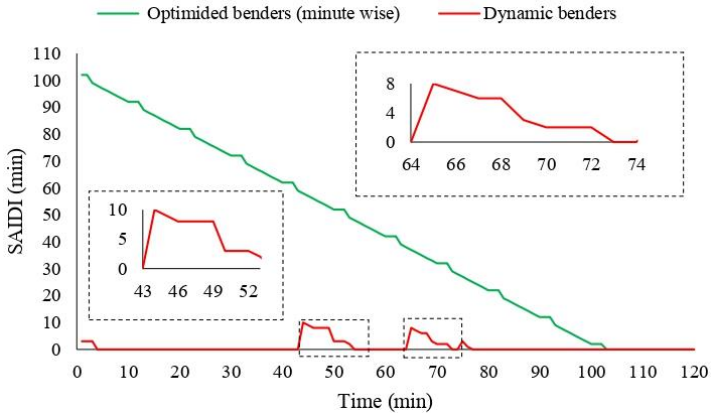

Figure 18: Minute-wise variation of SAIDI under cases 2(c) and 2(d)

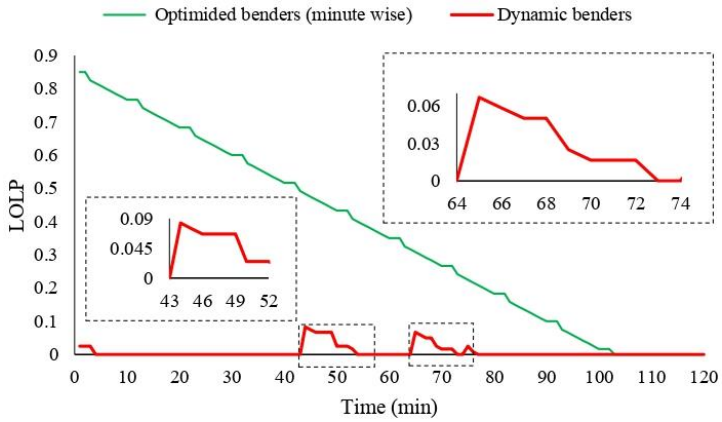

Figure 19: Minute-wise variation of LOLP under cases 2(c) and 2(d)

Figures 16, 17, 18, 19 represents the variation of reliability indices with optimised benders (minute-wise) and dynamic benders in Scenario 2 respectively. A fixed combination of 2 MWh battery and 2 MW PV determined through optimized Benders decomposition is sufficient to support a 10% grid outage. Thus, this combination is used to estimate reliability indices for optimised Benders (minute wise). Further, dynamic Benders is employed to estimate reliability indices by optimizing every possible PV and battery combination of grid outage through out the total journey. In Figures 16, 18, 19, the results shown in green colour reflect the minute wise optimised Benders decomposition approach i.e. case 2(c). The simulation results reveal that reliability indices are significantly higher during early outage periods. Further, the mean reliability indices namely EENS, SAIFI, SAIDI, LOLP are 4.2913, 1.0200, 43.2100, 0.3601 respectively under case 2(c) shown in the Table 2. It is important note that in the Table 2, the zero values of reliability indices observed in case 2(b) do not indicate that the system is fully reliable. This result is specific to a condition where grid outage is limited to 10% only.

Power System Technology
ISSN:1000-3673
Received: 16-11-2025 Revised: 05-12-2025 Accepted: 30-01-2026

The dynamic Benders is employed to estimate reliability indices by optimizing every possible PV and battery combination of grid outage through out the total journey. Thus, the mean reliability indices namely EENS, SAIFI, SAIDI, LOLP are 0.015, 0.5900, 0.8110, 0.0067 respectively showing substantial improvement compared with other cases as shown in the Table 2. Further, outages occurring within the intervals from 43 to 52 and 64 to 72 minutes exhibit non zero reliability indices as shown in Figures 16, 18, 19 with dotted lines. Besides, the variation is minimal, the EENS is below 0.2 MWh, SAIDI with in 10 minutes and LOLP limited to 0.066 respectively.

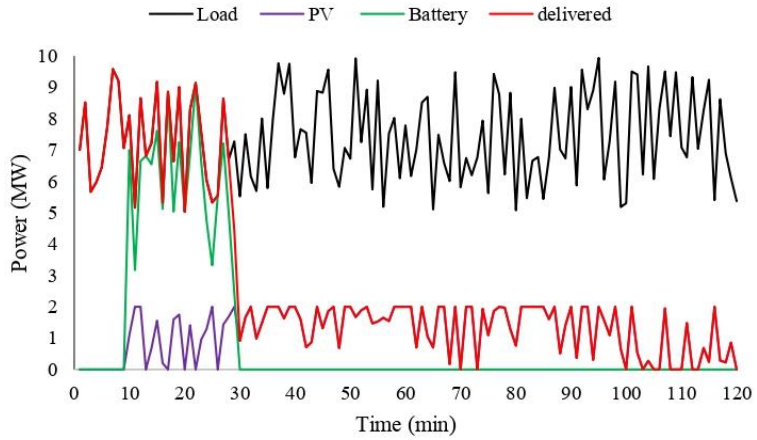

Figure 20: Power delivered by optimised Benders at t = 10th minute outage under Scenario 2

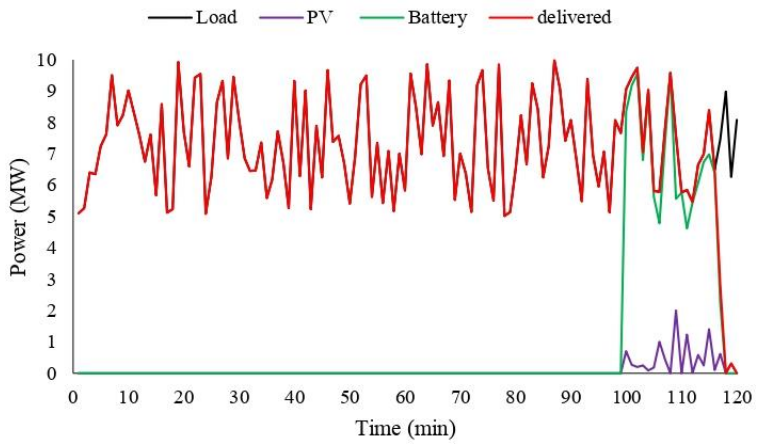

Figure 21: Power delivered by optimised Benders at t = 100th minute outage under Scenario 2

Interestingly, Figure 17 showcases that during certain part of journey, SAIFI of case 2(d) is higher compared with case 2(c). However, case 2(d) characteristics should not be viewed as a limitation, since the primary objective is to minimize EENS. Further, any one interruption in case 2(c) makes the train stop for entire journey is counted as one interruption and therefore it results higher EENS and lower SAIFI. But, case 2(d) exhibits multiple short duration

Power System Technology
ISSN:1000-3673
Received: 16-11-2025 Revised: 05-12-2025 Accepted: 30-01-2026

interruptions due to application of dynamic benders optimisation at each minute. It enables to operate the train through out the journey resulting higher SAIFI but lower EENS providing resilient energy service continuation to train. Although, case 2(d) mean SAIFI is 0.590, which is lower compared to case 2(c) i.e. 1.02 interruptions. Dynamic Benders in Case 2(d) adapts PV-battery sizing to each 10 minute segment, eliminating mismatch seen in Case 2(c). Thus, reduction of EENS, SAIFI, SAIDI, LOLP are 99.65%, 42.15%, 98.12%, 98.16% respectively.

Figures 20, 21 visualises the incomplete power supply under grid outage at 10^{th} and 100^{th} minutes by minute-wise optimised Benders approach. The 2 MWh battery and 2 MW PV combination obtained from case 2(b) are utilised to support during grid outage. Figure 20 reveal that an outage initiated at 10^{th} minute experiences unmet demand from 29^{th} minute to the end of the journey. Similarly, when the outage starting at the 100^{th} minute, the load remains unserved from the 117^{th} minute onward as shown in Figure 21.

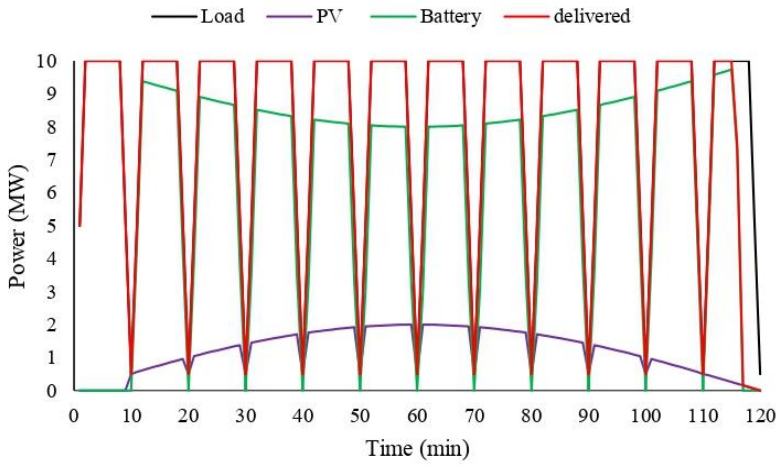

Figure 22: Power delivered by dynamic Benders at t = 10^{th} minute outage under Scenario 2

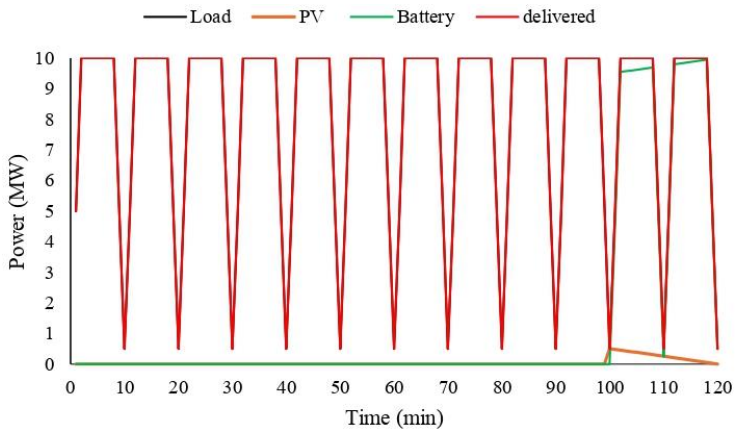

Figure 23: Power delivered by dynamic Benders at t = 100^{th} minute outage under Scenario 2

Power System Technology
ISSN:1000-3673
Received: 16-11-2025 Revised: 05-12-2025 Accepted: 30-01-2026

Figures 22, 23 illustrates the simulation model capturing the battery and PV power contributions under dynamic Benders (case 2(d)) during outages occurring at 10th and 100th minutes respectively. Interestingly, it is observed that maximum power has been delivered under both outage occurrences at 10th and 100th minute. Dynamic Benders optimisation visualises the energy dispatch requirements under the minute wise outage sensitivity is the reason for delivering the power. Further, Figure 22 illustrates the battery and PV power contribution from 10th to 115th minute and later on load is unserved. However, this is not a serious concern as the EENS constraint was allowable upto 0.2 MWh and whereas Figure 20 met the demand upto 29th minute only. Furthermore, it is observed that in the event of an outage at 100th minute, the battery and PV systems support the complete delivery of power as shown in Figure 23. Besides, the battery contributes maximum demand compared to PV since dynamic bender reallocates energy based on cost effectiveness. Moreover, the proposed work work analyses how the solar availability variations, load profile and outage timings influence optimal energy dispatch strategy. Thus, the optimised PV and battery combinations obtained from dynamic Benders aids in real time energy management strategy to support the bullet train under grid outage scenarios.

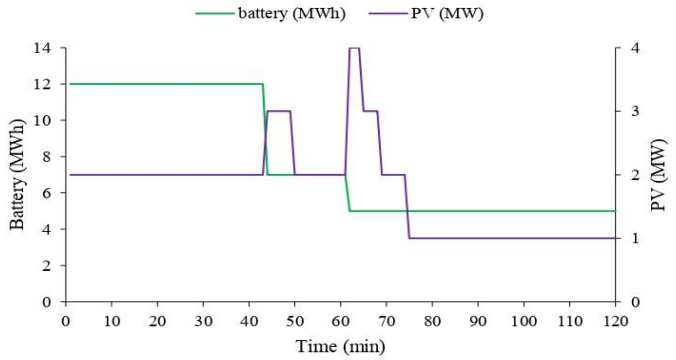

Figure 24: Optimised battery and PV sizing under Scenario 2

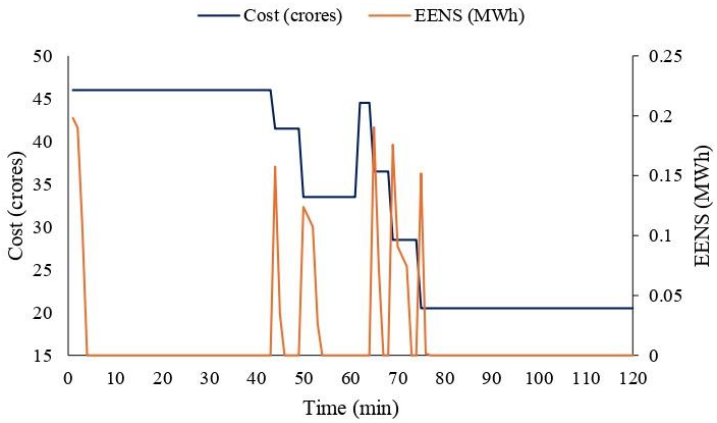

Figure 25: Trade-off between cost and EENS under Scenario 2

Power System Technology
ISSN:1000-3673
Received: 16-11-2025 Revised: 05-12-2025 Accepted: 30-01-2026

Figures 24, 25 intercept the cost and reliability trade off with varying battery and PV sizes under dynamic Benders approach. When the outage occurring between 1 to 43 minutes, the battery and PV sizing was found to be 12 MWh and 2 MW respectively incurring a cost of 46 crores. Further, the cost, battery and PV sizing was constant for respective durations of (1−43), (44 − 49), (50 − 61), (62 − 64), (65 − 68), (69 − 74), (75 − 120) minutes respectively. The dynamic Benders optimisation allocates single energy configuration having optimal capacity and cost to handle later outage duration with satisfying EENS constraint. For example, when an outage is initiated at 75th minute, the battery and PV capacity was estimated to be 5 MWh and 1 MW with a cost of 20.5 crores by the dynamic Benders. Later outages from 76th to 120th minutes utilise 5 MWh and 1 MW as it does not violate EENS constraint which is guaranteed to handle worst case scenarios.

The main advantage of dynamic Benders i.e case 2(d) under Scenario 2 has been explained by an example. If a bullet train loses power at a given segment, the master problem evaluates the battery and PV requirement for supporting energy to complete remaining journey of the considered segment. Then the sub problem decides the energy dispatch needed by battery and PV at ideal solar and load profiles. Thus, bi-level optimisation evaluates optimal sizing and cost under grid outages.

4.3. Scenario 3: Joint Cost Reliability MILP Framework

In this scenario, a grid outage covering 10% of the total 120 minute train journey was considered to evaluate system reliability. Accordingly, outage events were introduced at minutes 2, 10, 16, 17, 19, 26, 29, 39 48, 59, 60, 96 respectively. These selected outage intervals are distributed across the journey to simulate realistic grid outages enabling assessment of joint cost and reliability. Further, the segmented train load profile and ideal solar PV profile are considered for Scenario 3 respectively. After performing MILP optimisation, the optimal battery and PV capacity were 0.5 MW and 1.03 MWh respectively incurring 6.5 crores cost.

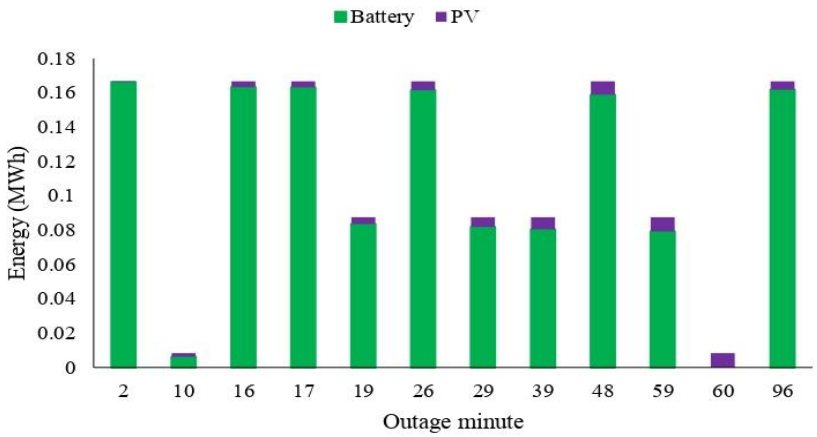

Figure 26: Energy support of battery and PV by MILP under Scenario 3

Power System Technology
ISSN:1000-3673
Received: 16-11-2025 Revised: 05-12-2025 Accepted: 30-01-2026

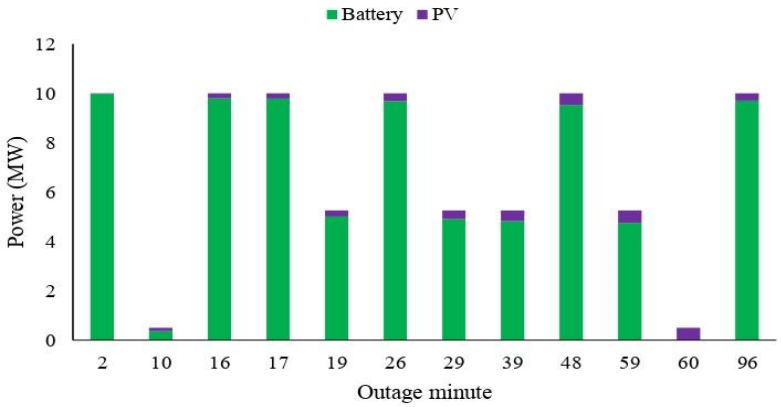

Figure 27: Power delivered by battery and PV by MILP under Scenario 3

Figures 26 and 27 illustrates the energy supported and power delivered during outage periods through MILP technique. It was revealed that outages at minutes 2, 16, 17, 26, 48, 96 were supplied by battery and PV systems contributing equal power (MW) or energy (MWh). Further, these time points align with the cruise phase of the train's load profile, where the demand remains constant enabling balanced energy sharing. Further, same pattern has been followed for outage at 10, 60 minutes falling under deceleration phase and during 19, 29, 39, 59 minutes corresponding to acceleration phase of train's load cycle. The identical train load demand and the optimal equal PV and battery dispatch are reasons for the repeated estimated values. The optimised dispatch provided by MILP represents the system sizing calibration utilised to handle recurrent outage scenarios. Optimal battery and PV sizing is designed for arbitrary outages based on representative set of periodical operational load patterns of the bullet train. Thus, the accurate estimation of PV generation and battery requirement under acceleration, cruise, deceleration phases of train load profile are reflected by this methodology.

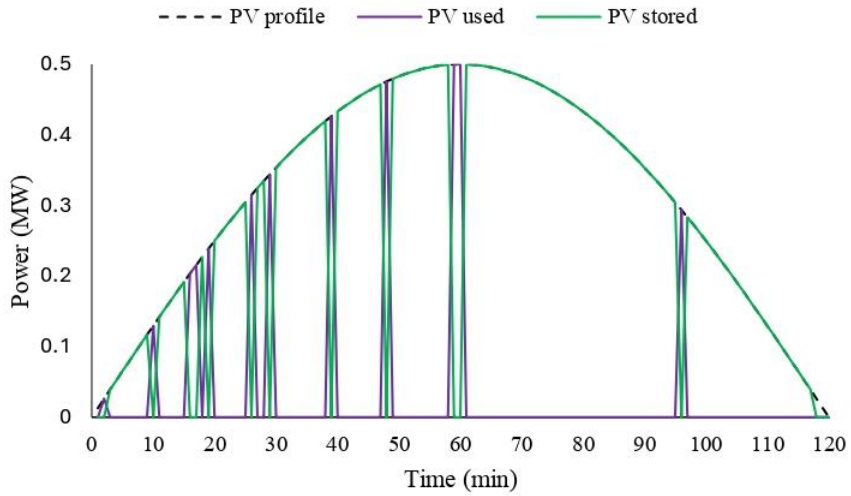

Figure 28: PV analysis of Scenario 3

Power System Technology
ISSN:1000-3673
Received: 16-11-2025 Revised: 05-12-2025 Accepted: 30-01-2026

Figure 28 visualises the PV generation profile, utilisation and capability to store surplus energy when PV supply exceeds load demand. The PV profile represented by the black dotted curve, follows a sinusoidal pattern peaking at 0.5 MW around 60th minute corresponding to mid point of journey. During blackout period, the optimisation strategy allocates PV energy to supply the train load. Further, during no outage period, the PV energy has been routed towards battery storage. Figure 28 explains during outage minutes such as 2, 10, 16, the PV contributes load with 0.0261, 0.1294, 0.2033 MW respectively. Besides, during no outage minutes such as 4, 11, 18, excess PV energy is stored, capable to deliver 0.0522, 0.1420, 0.1294, 0.2260 MW respectively under blackout periods.

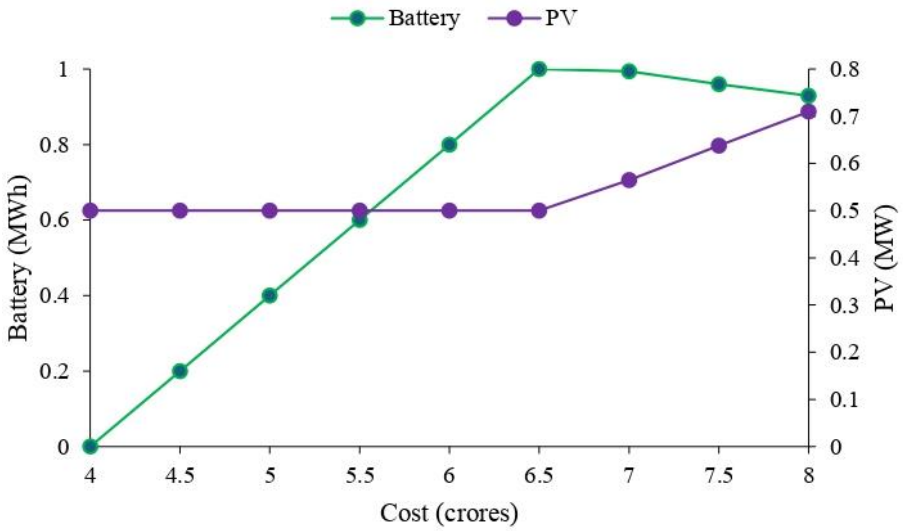

Figure 29: Cost constrained battery and PV sizing under Scenario 3

A cost constrained MILP optimisation approach is employed to identify the optimal PV and battery sizing to meet reliability requirements within a pre-defined budget. Further, MILP framework is solved at each budget level with the primary objective of minimising EENS. Figure 29 showcases the PV and battery sizing under different varying cost levels. The simulation results reveal that when the budget varies from 4 to 6.5 crores, the PV sizing was found to be 0.5 MW. Upon increasing the cost level to 8 crores, the PV sizing was increased to 0.7 MW since the optimiser has leverage to spend budget. Further, the battery sizing increases up to 6.5 crores and later it follows non monotonic behaviour from 6.5 to 8 crores. This phenomenon arises as the optimization strategy shifts towards PV generation rather than utilising battery storage to support load demand without compromising reliability performance. Table 3 lists the reliability indices with varying budget levels. As the cost increases from 4 to 7 crores, the reliability indices are improved especially EENS decreases from 1.3055 to 0 MWh respectively. Thus, cost constrained MILP optimisation framework ensures optimal trade- off between reliability objectives and economic constraints.

Power System Technology
ISSN:1000-3673
Received: 16-11-2025 Revised: 05-12-2025 Accepted: 30-01-2026

Table 3: Cost Constrained Reliability Indices under Scenario 3

Cost (crores)	EENS (MWh)	SAIFI (Int)	SAIDI (min)	LOLP
4	1.3055	10	11	0.0197
5	0.5680	4	5	0.0470
6	0.2085	2	2	0.0167
7	0.0000	0	0	0.0000

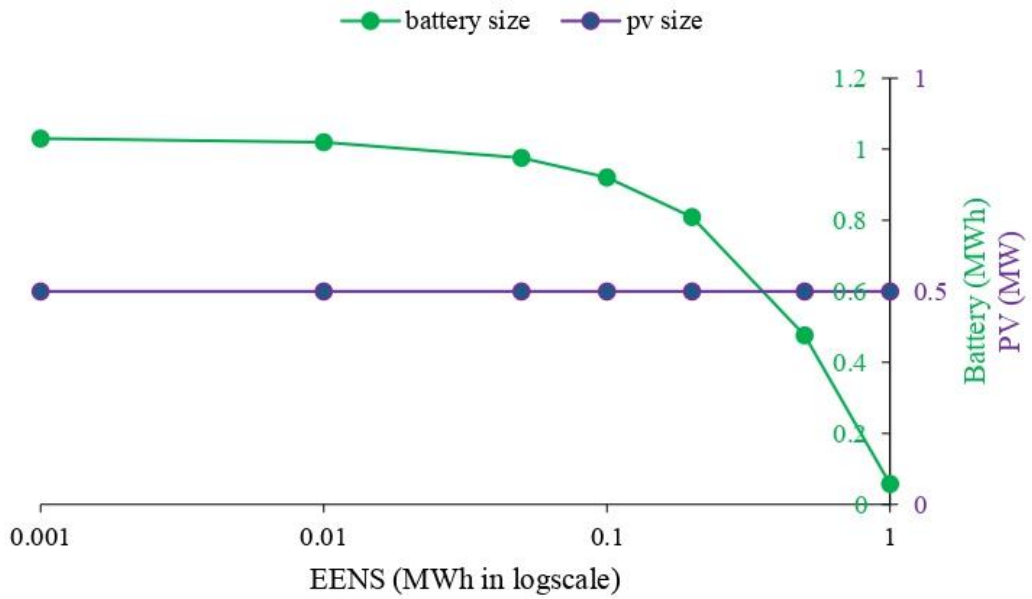

Figure 30: EENS constrained battery and PV sizing under Scenario 3

Table 4: EENS Constrained Reliability Indices under Scenario 3

EENS (MWh)	Cost (crores)	SAIFI (Int)	SAIDI (min)	LOLP
0.001	6.575	1	1	0.0083
0.010	6.550	1	1	0.0083
0.500	6.020	2	2	0.0167
1.000	4.140	9	10	0.0830

Power System Technology
ISSN:1000-3673
Received: 16-11-2025 Revised: 05-12-2025 Accepted: 30-01-2026

Besides, the cost reliability trade-off can be effectively addressed by minimising the total system cost subjected to EENS constraints. Therefore, MILP is solved at each EENS constraint to minimise the cost. As shown in Figure 30, the EENS constraints are varied from 0.001 MWh to 1 MWh, the system relies on battery range from 0.579 MWh to 1.03 MWh, while the PV capacity remains constant at 0.5 MW. Further, Table 4 lists the EENS constrained reliability indices. As the EENS constraints are relaxed from 0.001 MWh to 1 MWh, the cost decreased from 6.575 crores to 4.140 crores. Since the optimizer has the flexibility to allocating budget for additional PV or battery capacity, the reliability indices are improved for higher budget and deteriorated for lower budget. The main advantage of joint cost reliability MILP framework has been explained with an example. The proposed joint MILP formulation incorporating both cost and EENS constraints acts as a valuable tool for financial stakeholders and power system energy planners.

5. Conclusion

This paper proposes a unified optimisation framework for reliability driven energy management of high speed bullet trains operating under grid outage conditions. Scenarios 1 and 2 are characterized by stochastic and segment based load and solar profile modeling, respectively. Benders decomposition enables adaptive PV-battery resizing, while MILP (Mixed Integer Linear Programming) quanties the cost reliability trade-off. In Scenarios 1 and 2, dynamic Benders re-optimisation at each outage minute outperformed fixed optimised sizing, demonstrating the significance of adaptive renewable scheduling under both stochastic and segment based operating conditions. Scenario 3 is chracterisezed by joint cost reliability trade-off. Further, Scenario 3 is evaluated by MILP highlight that relaxing budget limits progressively enhances reliability and enables feasible renewable sizing. The integrated framework therefore supports reliability driven PV-battery scheduling that mitigates energy deficits and improves system robustness during outages. Collectively, the study unifies outage modelling, adaptive renewable sizing and cost aware reliability optimisation into a coherent and scalable decision support methodology for bullet train systems.

Refrences

[1] S. Su, and et al, “A Data-Driven Iterative Learning Approach for Optimizing the Train Control Strategy,” *IEEE Trans on Industrial Informatics*, vol. 19, pp. 7885-7893, 2023.

[2] L. Ning, and et al, “Deep Deterministic Policy Gradient for High Speed Train Trajectory Optimization,” *IEEE Transactions on Intelligent Transportation Systems*, vol. 23, no. 8, pp. 11562-11574, 2022.

[3] W. Zheng, and et al, “A Systematic Approach to the High-Level Maintenance Scheduling for High-Speed Trains in China,” *IEEE Tran on Reliability*, vol. 73, pp. 142-155, 2024.

Power System Technology
ISSN:1000-3673
Received: 16-11-2025 Revised: 05-12-2025 Accepted: 30-01-2026

[4] T. Men, and et al, "Reliability Modeling and Parameter Estimation for High-Speed Train Wheels Subject to Multi-Dimensional Degradation Processes Considering Mutual Dependency," *IEEE Transactions on Reliability*, vol. 73, no. 2, pp. 1325-1340, 2024.
[5] S. Hasanzadeh, S. F. Zarei and E. Naja, "A Train Scheduling for Energy Optimization: Tehran Metro System as a Case Study," *IEEE Trans. On Intelligent Transportation Systems*, vol. 24, no. 1, pp. 357-366, 2023.
[6] H. Yu, and et al, "Power System Optimal Dispatch Integrating the Responsive High-Speed Train Fleet," *IEEE Transactions on Smart Grid*, vol. 16, no. 1, pp. 728-740, 2025.
[7] Gokula Manikandan , and et al, "The positive and negative impact of novel utility demand response programme and stochastic utility-driven events on renewable penetration and flexibility activation of train and station systems," *Sustainable Energy, Grids and Networks*, vol. 37, 101258, ISSN 2352-4677, 2024.
[8] A. Ruvio , and et al, "MILP based optimization tool for PV and BESS planning in railways: a case study in extensive market analysis," *Sustainable Energy, Grids and Networks*, vol. 44, 102063, ISSN 2352-4677, 2025
[9] Z. Tian, and et al, "Integration of Energy Storage and Renewable Energy Sources into AC Railway System to Reduce Carbon Emission and Energy Cost," *IEEE Vehicle Power and Propulsion Conference (VPPC)*, 2020.
[10] T. Lavanya, and et al, "Energy Management Strategy for Grid-Tied Photovoltaic Systems with Integrated Hybrid Energy Storage," *Power System Technology*, vol. 48, no. 1 2024.
[11] C. Cheng, and et al, "Enhanced Fault Diagnosis Using Broad Learning for Traction Systems in High-Speed Trains," *IEEE Transactions on Power Electronics*, vol. 36, no. 7, pp. 7461-7469, 2021.
[12] J. A. Aguado, and et al, "Optimal Operation of Electric Railways With Renewable Energy and Electric Storage Systems," *IEEE Trans. on Smart Grid*, vol. 9, pp. 993-1001, 2018.
[13] T. Lavanya, and et al, "Energy Management Strategy for Grid-Tied Photovoltaic Systems with Integrated Hybrid Energy Storage," *Power System Technology*, vol. 48, no. 1, 2024.
[14] Li Lin, and et al, "Train regenerative braking energy management strategy considering battery state of charge," *Sustainable Energy, Grids and Networks*, vol. 43, 101786, ISSN 2352-4677, 2025.
[15] Y. Liu, and et al, "Robust Energy Management of High-Speed Railway Co-Phase Traction Substation With Uncertain PV Generation and Traction Load," *IEEE Transactions on Intelligent Transportation Systems*, vol. 23, no. 6, pp. 5079-5091, 2022.
[16] A. Zhou, R. Yan and T. K. Saha, "Capacity and Control Strategy Design of Isolated Micro-Grid With High Renewable Penetration," *IEEE Transactions on Sustainable Energy*, vol. 11, no. 3, pp. 1173-1184, 2020.

Power System Technology
ISSN:1000-3673
Received: 16-11-2025 Revised: 05-12-2025 Accepted: 30-01-2026

[17] C. Huang, and et al, "Demand Response for Industrial Micro-Grid Considering Photovoltaic Power Uncertainty and Battery Operational Cost," *IEEE Trans. on Smart Grid*, vol. 12, no. 4, pp. 3043-3055, 2021.
[18] M. Javadi, and et al, "Frequency Stability Constrained BESS Sizing Model for Microgrids," *IEEE Trans. on Power Systems*, vol. 39, no. 2, pp. 2866-2878, 2024.
[19] Y. Sun, and et al, "Multitime Scale Optimization of Urban Micro-Grids Considering High Penetration of PVs and Heterogeneous Energy Storage Systems," *IEEE Internet of Things Journal*, vol. 11, no. 14, pp. 24428- 24438, 2024.
[20] Y. Li and J. Wu, "Optimum Integration of Solar Energy With Battery Energy Storage Systems," *IEEE Trans. on Engineering Management*, vol. 69, no. 3, pp. 697-707, 2022.
[21] Thiago Gomes, and et al, "Reliability Improvement on Power Distribution Systems by Network Reconfiguration: A Matheuristic Approach to Clustering Electrical Consumers," *Power System Technology*, vol. 49, no. 3, 2025.
[22] M. Du, and et al, "Reliability Evaluation of Generation and Transmission System Considering Direct Power Purchase by Large Consumers," *Power System Technology*, vol. 43, no. 2, 2019.
[23] V. Swapna and M. T. L. Gayatri, "Power Quality Issues of Grid Integration of Distributed Generation: A Review," *International Conference on Computational Performance Evaluation (ComPE)*, pp.142-147, 2021.
[24] M. S. Alvarez-Alvarado, and et al, "Power System Reliability and Maintenance Evolution: A Critical Review and Future Perspectives," *IEEE Access*, vol. 10, no. 5, pp. 51922-51950, 2022.
[25] T. Zhang, and et al, "Analytical Calculation Method of Reliability Sensitivity Indexes for Distribution Systems Based on Fault Incidence Matrix," *Journal of Modern Power Systems and Clean Energy*, vol. 8, no. 2, pp. 325-333, 2020.
[26] K. Zou, and et al, "Distribution System Restoration With Renewable Resources for Reliability Improvement Under System Uncertainties," *IEEE Trans. on Industrial Electronics*, vol. 67, no. 10, pp. 8438-8449, 2020.
[27] P. V. R. Varma and S. A-julla, "Assessment of Reliability Indices under Generation and Peak Load Constrained Scenarios," *IEEE Int. Conference on SEFET*, India, 2023.
[28] W. Liu, and et al, "Analytical Reliability Evaluation of Active Distribution Systems Considering Information Link Failures," *IEEE Transactions on Power Systems*, vol. 35, no. 6, pp. 4167-4179, 2020.
[29] Pikkin Lau, and et al, "A Coalitional Cyber-Insurance Design Considering Power System Reliability and Cyber Vulnerability," *IEEE Trans. on Power Systems*, vol. 36, no. 6, pp. 5512-5524, 2021.
[30] Pikkin Lau, and et al, "A Novel Mutual Insurance Model for Hedging Against Cyber Risks in Power Systems Deploying Smart Technologies," *IEEE Trans. on Power Systems*, vol. 38, no. 1, pp. 630-642, 2023.